

Full Length Research Paper

Preparation of MWCNT/Ba_{0.2}Sr_{0.2}La_{0.6}MnO₃/PANI nanocomposites and investigation of its electromagnetic properties in KU-band

S. H. Hosseini^{1,5*}, R. Paymanfar², T. Afshari³ and S. S. Hosseini⁴

¹Department of Chemistry, Faculty of Science, Islamshahr Branch, Islamic Azad University, Tehran, Iran.

²Department of Chemistry, Faculty of Technical and Engineering, Saveh Branch, Islamic Azad University, Saveh, Iran.

³Department of Physical Chemistry, Faculty of Chemistry, University of Kashan, Kashan, Iran.

⁴Faculty of Veterinary Medicine, Science and Research Branch, Islamic Azad University, Tehran-Iran.

⁵Nika Pooyesh Strategic Sciences Research Institute, NBP Economic Group, Tehran-Iran.

Received 17 August, 2020; Accepted 16 September, 2020

The aim of this study was enhanced the absorption of electromagnetic waves by nanocomposite containing polyaniline (PANI), functionalized multi wall carbon nanotubes (MWCNTs) in the presence of magnetic Ba_{0.2}Sr_{0.2}La_{0.6}MnO₃ nanoparticles (NPs). At First MWCNTs was functionalized by 3:1 ratio of sulfuric and nitric acid, then functionalized MWCNTs was coated by NPs with the traditional sol-gel method. In the final step, MWCNTs/NPs covered by PANI with an in situ polymerization in an aqueous solution. FESEM, XRD, vibrating sample magnetometer (VSM), FTIR analysis was confirmed NPs synthesis in appropriate size and shape and functionalized MWCNTs was coated with NPs and PANI synthesized by correct chemical formula covered all of them, too. The maximum reflection loss of the Ba_{0.2}Sr_{0.2}La_{0.6}MnO₃ NPs and MWCNT/Ba_{0.2}Sr_{0.2}La_{0.6}MnO₃ were about -12.04dB at 14.82 GHz and -22.36 dB at 14.78GHz with a bandwidth of 2.67GHz (more than -10dB). The conclusion indicated we could good microwave shielding in KU-band (12-18 GHz) by these nanocomposites.

Key words: Multiwall carbon nanotube, microwave absorption, magnetic nanoparticles, polyaniline.

INTRODUCTION

The study of microwave absorption in 8 to 18 GHz has received much attention in recent years. Therefore, the crystal structure of the magnetic nanoparticles according to their constituent elements and magnetic properties of nanoparticles is effective in electromagnetic interfering (EMI) and electromagnetic wave absorber. Magnetic

nanoparticles are produced in various ways such as chemical co-precipitation (Hosseini and Zamani, 2016a), sol-gel combustion (Amiri, 2019), hydrothermal synthesis (Gomez et al., 2019), solid state (Ban et al., 2018) and spray pyrolysis (Minin et al., 2018). Magnetic nanoparticles alone have disadvantages such as low

*Corresponding author. E-mail: dr.shhosseini@gmail.com.

peak width microwave absorption in 8 to 18 GHz region. By regulating the addition of iron source, different magnetic contents and Co:Fe molar ratios of graphene oxide/carbon nanotubes/CoxFe_{3-x}O₄ ternary nanocomposites could be selectively synthesized by Mei and one-step hydrothermal method (Mei et al., 2020) and could be applied to design high performance microwave absorbers. Carbon nano-types have features such as morphology in nano-endurance and high resistance and suitable surface to volume ratio of the electric and magnetic properties (electrical permeability factor) and high permittivity (Rao et al., 2018). One of their important features is surface function that makes them very suitable for the sensor (Bezzon et al., 2019). Eddy current loss natural resonance, size and shape factors, and the advances and performance review in microwave absorption (e.g., absorption bandwidth, reflection loss values, absorption peak position) using various nanomaterials, such as carbon nanotubes, carbon fibers, graphenes, oxides, sulfides, phosphides, carbides, polymers and metal organic frameworks (Green and Xiaobo, 2019). Recently, a broadband perfect meta material absorber on FR-4 epoxy substrate for X-band and Ku band applications is proposed by Sen et al. (2017). The absorption bandwidth covers the entire X and Ku bands of operation with more than 85% absorption over the range. Acharya and Datar (2020) prepared wideband (8-18 GHz) microwave multi absorber using copper aluminium ferrite and reduced graphene oxide in polymer matrix.

Conductive polymers have been considered in EMI magnetic interfering rechargeable batteries, catalysts and sensors and electrodes and various other fields (Mishra, 2018; Ibanez et al., 2018). Conductive polymer can be used with magnetic nanoparticles in EMI magnetic interfering to increase the width of the frequency absorption of the 8 to 18 GHz waves. Between the conductive polymer, polyaniline (PANI) and PPy have attracts attention due to its chemical and physical properties of electro-chemical as well as provide an easy method of preparation. Recently, several methods were used for the CNT in polymers such as mixing solution and use of suspension of CNT dissolved in the polymer as film casting (Biswas et al., 2020). The polymerization simultaneously using a mixture of CNT and mixed monomer-polymer case (Donescu et al., 2017) and mixed mechanically polymer melts with CNT (Banerjee and Dutta, 2019).

In preceding works, we have synthesized some papers of electromagnetic absorbing materials (Hosseini et al., 2016b) based on conducting polymers and nanoparticles. Although some other works on such composites for neutron attenuation (Hosseini et al., 2020a) and multi absorbers (Dolabi et al., 2020; Hosseini et al., 2020b) based on conducting polymers in recent years have been reported, too. In this research, we have tried to make

new NPs with special interest.

METHODOLOGY

Materials

The multiwall carbon nanotube (MWCNT) with outer diameter: 10-20 nm and 30 μ m length and 200 m²/g special surface area purity 95% was purchased from Neutrino company. All of the other chemical materials such as sulfuric acid 98%, nitric acid 65%, methylmethacrylate monomer, toluene, benzoyl peroxide, methanol, Mn(NO₃)₂.4H₂O, Ba(NO₃)₂, Sr(NO₃)₂, LaN₃O₉.6H₂O, citric acid (C₆H₈O₇.H₂O), NH₃, urea, aniline monomer, ammonium persulfate (APS) from MERCK and dodecylbenzenesulfonic acid solution (DBSA) from SIGMA-ALDRICH were purchased.

Characterization

Ultrasonic experiments were carried out in a BANELIN ultrasonic disperser SONOREX DIGITEC DT 255 H, XRD patterns for the samples were recorded on a Philips PW1800 instrument with Cu K α radiation (0.15418 nm) operating at 40 kV and 30 mA for the 2 θ range 4 to 90 with scan steps of 0.02. The average crystallite size and shape can be calculated according to the Debye-Scherrer formula using XRD data and electron microscopy images, respectively. Field-emission scanning electron microscopy (FESEM) was performed on a Hitachi S-4160 instrument to observe the surface morphology of the nanoparticles and nanocomposites. IR curves were prepared using a Perkin Elmer RX1 FT-IR. Clear tablets were made using KBr salt and 15 tone machine to identify links and functional groups present in the samples. Magnetic measurements were carried out at room temperature in the applied field range from -10000 to +10000 Oe at a vibrating frequency of 25 Hz using an IRI Kashan (IRAN) vibrating sample magnetometer (VSM). The microwave absorption properties of the nanocomposites were measured at room temperature using a microwave vector network analyzer (Agilent Technologies, model HP 8510c) in the range 12 to 18 GHz.

Preparation of MWCNT/Ba_{0.2}Sr_{0.2}La_{0.6}MnO₃ nanocomposite (20%wt NPs)

MWCNT dispersed in mixture of concentrated sulfuric acid and nitric acid 3:1 by high power ultrasonic and mechanical stirring for 8 h for the functional group's carboxylic acid based on MWCNTs surface. Then suspension was washed with de-ionized water several times to reach neutral pH and dried for 12 h at a temperature 50°C. The enough amount of functionalized MWCNTs diffuse in de-ionized water by ultrasonic waves for 30 min. Ba, Sr, La and Mn nitrates in the appropriate de-ionized water by intense magnetic stirrer was dissolved according to stoichiometric ratio of metal Ba_{0.2}Sr_{0.2}La_{0.6}MnO₃. According to the molar ratio of 1:1 with metal cations, first the citric acid and then urea were added to a solution. The pH was adjusted to about 8 by adding ammonia solution. The hydrophilic absorbent cotton dipped in the sol as anti-agglomeration under magnetic stirring for 20 min and became gel at 80°C in oven. Then dried gel was produced at 250°C furnace for 24 h. Finally, the dried gel was obtained at 700°C for 4 h and fully calcined until magnetic nanoparticle grown to fit the shape of the shell of the carbon nanotubes.

Preparation of MWCNT/Ba_{0.2}Sr_{0.2}La_{0.6}MnO₃/PANI nanocomposite

Dodecyl benzene sulfonic acid (DBSA, 0.5 g) in 20 ml de-ionized

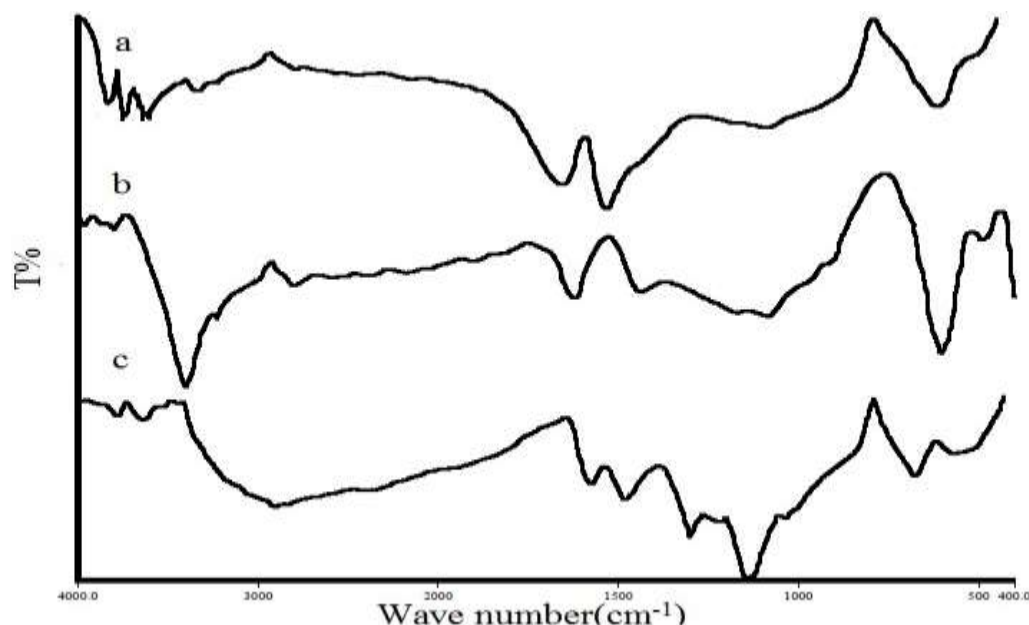


Figure 1. FT-IR spectra of (a) $\text{Ba}_{0.2}\text{Sr}_{0.2}\text{La}_{0.6}\text{MnO}_3$ NPs, (b) $\text{Ba}_{0.2}\text{Sr}_{0.2}\text{La}_{0.6}\text{MnO}_3/\text{MWCNT}$, and (c) $\text{Ba}_{0.2}\text{Sr}_{0.2}\text{La}_{0.6}\text{MnO}_3/\text{MWCNT}/\text{PANI}$ nanocomposites.

water was under vigorous mechanical stirring for 30 min to floor. Next 0.2 g of nanocomposites $\text{MWCNT}/\text{Ba}_{0.2}\text{Sr}_{0.2}\text{La}_{0.6}\text{MnO}_3$ was added simultaneously under mechanical stirring and ultrasonic waves for 20 min. Then 0.5 mL of fresh aniline with 5 mL of double distilled water was added to solution and placed under mechanical stirring and ultrasonic waves at 0 to 5°C. In the final step, 1.245 g of ammonium persulfate as initiator was dissolved in 10 mL water and drop by drop added to solution. After 2 h of sonic and intense mechanical stirring simultaneously at 0 to 5°C, PANI was covered by nanocomposite surface as well as by different weight ratio of $\text{MWCNT}/\text{Ba}_{0.2}\text{Sr}_{0.2}\text{La}_{0.6}\text{MnO}_3$.

Preparation microwave absorber of paraffin/composite

After melting paraffin at 250°C, nano material to requirement of wt% was dispersed here by ultrasonic for 10 s and molded as tablet shape.

RESULTS AND DISCUSSION

IR spectra

$\text{MWCNT}/\text{Ba}_{0.2}\text{Sr}_{0.2}\text{La}_{0.6}\text{MnO}_3/\text{PANI}$ is evaluated in Figure 1 at several steps of synthesis. The $\text{Ba}_{0.2}\text{Sr}_{0.2}\text{La}_{0.6}\text{MnO}_3$ NPs absorption peaks are as shown in Figure 1a. The broad peak at 607.82 cm^{-1} was attributed to metal oxides vibrations of Mn-O and La-O and Sr-O and Ba-O. The absorption peaks at 3600 and 1649.51 cm^{-1} were assigned to the stretching vibration of O-H and C=O bonds in citric acid that was bonded with NPs, respectively. In $\text{Ba}_{0.2}\text{Sr}_{0.2}\text{La}_{0.6}\text{MnO}_3/\text{MWCNT}$ spectrum is

as shown in Figure 1b, absorption peak at 603.84 cm^{-1} was related to metal oxides rocking vibrations such as Mn-O and La-O and Sr-O and Ba-O. Two peaks at 1621.03 and 3404.42 cm^{-1} were attributed to C=O and O-H stretching vibration, respectively and confirm MWCNTs were functionalized and carboxylic acid is based on them. The broad absorption peak at 1089.38 cm^{-1} is assigned to stretching vibration of C-O on carbon nanotubes.

Finally, Figure 1c shows infrared spectrum of nanocomposite $\text{Ba}_{0.2}\text{Sr}_{0.2}\text{La}_{0.6}\text{MnO}_3/\text{MWCNT}/\text{PANI}$, absorption peak at 675.76 cm^{-1} was related to lanthanum strontium barium and manganese metal oxides rocking vibrations that show Mn-O, La-O and Sr-O and Ba-O bonds as a broad peak. Twin absorption peak at 1480.74 cm^{-1} was assigned to C=C stretching vibration in quinoid and benzenoid PANI rings. Absorption at 1299.75 cm^{-1} was attributed to the bending vibration of N-H and C-N stretching vibration for asymmetric carbon of benzenoid and secondary aromatic amine, strong absorption peak at 1142.63 cm^{-1} was assigned to N=Q=N stretching that Q refers to the quinonic-type rings and show the PANI covered another material. Two peaks at 1000 to 1100 cm^{-1} were related to C-O and S=O stretching vibration for remaining sulfonic acid and finally, two absorption peaks at 2750 to 3000 cm^{-1} were attributed to the C-H stretching vibration.

Infrared Spectroscopy of pristine multiwall carbon nanotube (MWCNT) and functionalized MWCNT was compared in Figure 2, too. In pristine MWCNT is as shown in Figure 2a, peak at 1200 region was assigned to

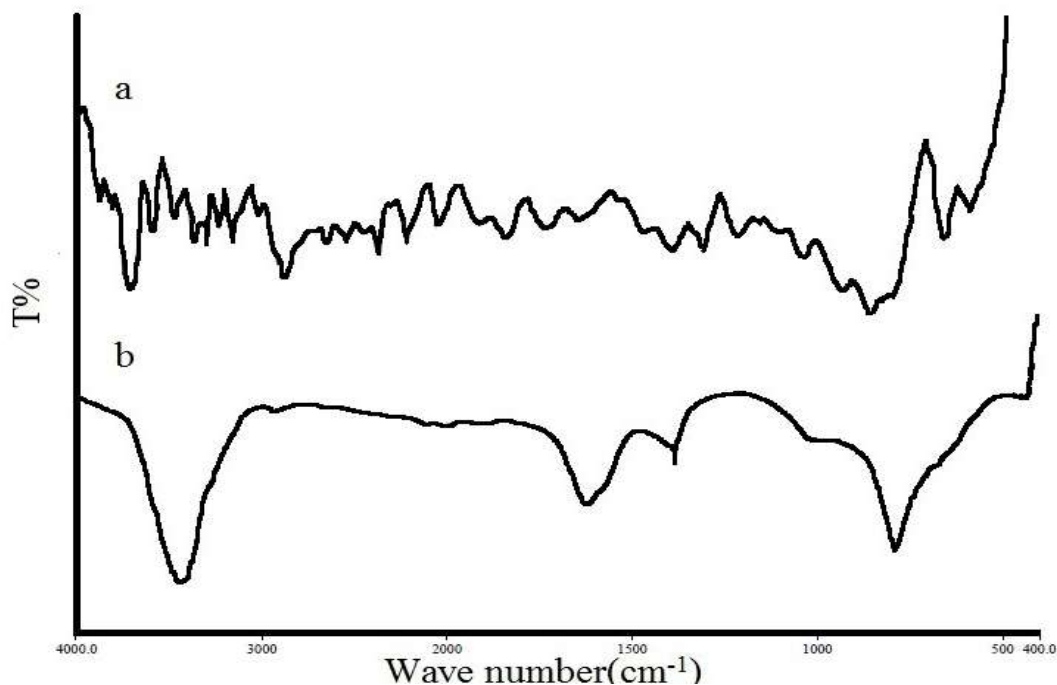


Figure 2. FT-IR spectra of the pristine (a) multiwall carbon nanotube and (b) functionalized MWCNT.

C-C stretching and maybe the peak at 2850 to 3000 cm^{-1} was related to stretching vibration of C-H and 1350 to 1480 was attributed to bending vibration of the C-H bond. Figure 2b shows the spectra of functionalized nanotubes, two absorption peaks at 3438.01 and 1614.83 cm^{-1} show O-H and C=O stretching vibrations in carboxylic acid based on carbon nanotubes and confirm MWCNTs surface was functionalized. At 1383.71 cm^{-1} , bending CH_3 absorption peak was placed ends of the nanotubes. Absorption peak at 793.61 cm^{-1} was attributed to the out-of-plane deformation vibration of the p-di-substituted carbon rings in the nanotube.

X-ray diffraction analysis

The XRD patterns of the $\text{Ba}_{0.2}\text{Sr}_{0.2}\text{La}_{0.6}\text{MnO}_3$ and $\text{MWCNT}/\text{Ba}_{0.2}\text{Sr}_{0.2}\text{La}_{0.6}\text{MnO}_3$ and $\text{MWCNT}/\text{Ba}_{0.2}\text{Sr}_{0.2}\text{La}_{0.6}\text{MnO}_3/\text{PANI}$ composites at $2\theta=0-80$ degrees are as shown in Figure 3a and c. In MWCNT/NPs and $\text{MWCNT}/\text{NPs}/\text{PANI}$ pattern, diffraction peaks about $2\theta=26$ was confirmed by (00-026-1080) card number according to (002) crystal plane. This result suggests that nanotubes structure has not been destroyed after coating by $\text{Ba}_{0.2}\text{Sr}_{0.2}\text{La}_{0.6}\text{MnO}_3$ and PANI. The diffraction peaks for $\text{Ba}_{0.2}\text{Sr}_{0.2}\text{La}_{0.6}\text{MnO}_3$ at $2\theta=32.65$ (110,104), 40.22 (202), 46.79 (024), 58.13 (030,214) were confirmed and show $\text{Ba}_{0.2}\text{Sr}_{0.2}\text{La}_{0.6}\text{MnO}_3$ nanoparticles were formed in accordance with the standard

card [98-005-7076] corresponding to crystal planes in the hexagonal structure. The average particle size of crystalline magnetite nanoparticles $\text{Ba}_{0.2}\text{Sr}_{0.2}\text{La}_{0.6}\text{MnO}_3$ calculated by the Scherer formula was equal to 21.7 nm. In MWCNT/NPs composite, CNT peaks have lesser intensity, due to the high proportion of magnetic NPs in composites. The results indicate that the traditional sol-gel method has no effect on crystals shape and nanocomposites form. The presence of carbon nanotubes is evident in all orientations (Figure 3b and c). In traditional sol-gel method, due to full coverage of nanotubes and sharp peaks at $30-40^\circ$ that was related to hexagonal crystalline structure than polymeric CNTs structure, make MWCNT peaks weak. XRD pattern of $\text{MWCNT}/\text{Ba}_{0.2}\text{Sr}_{0.2}\text{La}_{0.6}\text{MnO}_3/\text{PANI}$ nanocomposite is as shown in Figure 3c. The PANI shows two broad diffraction peaks at $2\theta=25.28$ and 20.6 which can be ascribed to the periodicity parallel and perpendicular to the polymer chains. It was indicated that $\text{MWCNT}/\text{Ba}_{0.2}\text{Sr}_{0.2}\text{La}_{0.6}\text{MnO}_3$ NPs can be incorporated in the PANI composites by the *in situ* polymerization method. According to XRD, NPs are formed on nanotubes by molar ratio and suitable size and shape.

FESEM analysis

FESEM of all steps in the synthesis of $\text{MWCNT}/\text{Ba}_{0.2}\text{Sr}_{0.2}\text{La}_{0.6}\text{MnO}_3/\text{PANI}$ nanocomposites are as shown

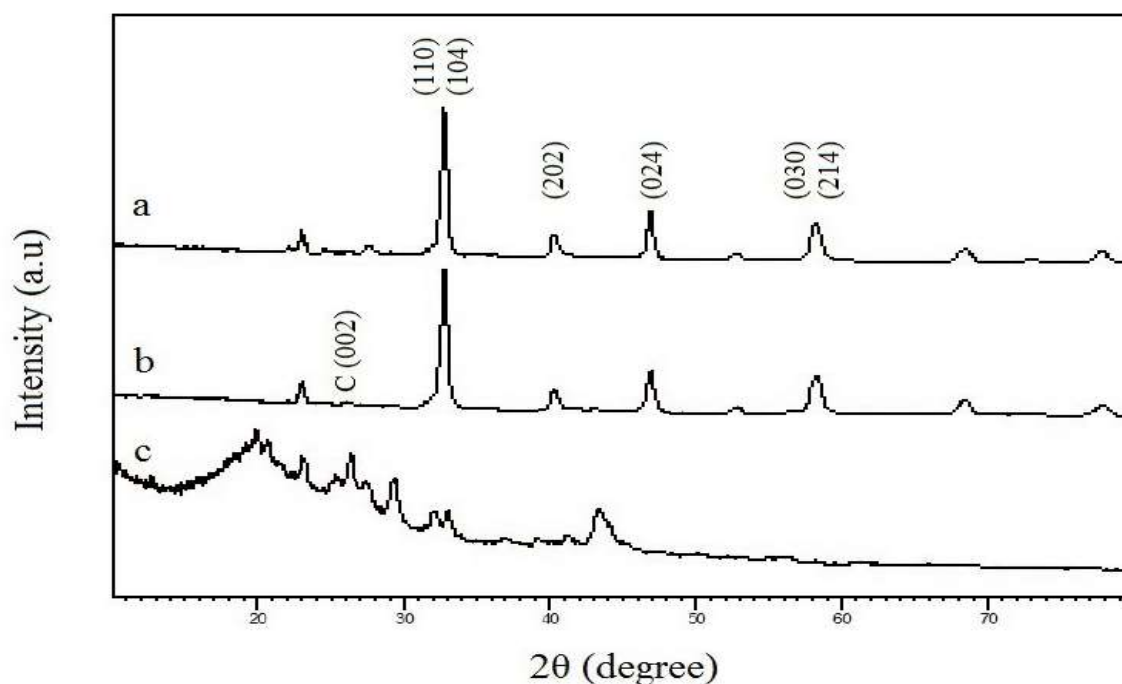


Figure 3. X-ray diffraction patterns of the (a) $\text{Ba}_{0.2}\text{Sr}_{0.2}\text{La}_{0.6}\text{MnO}_3$ NPs, (b) MWCNT/ $\text{Ba}_{0.2}\text{Sr}_{0.2}\text{La}_{0.6}\text{MnO}_3$ and (c) MWCNT/ $\text{Ba}_{0.2}\text{Sr}_{0.2}\text{La}_{0.6}\text{MnO}_3$ /PANI nanocomposites.

in Figure 4a and c. Hexagonal morphology and nanoparticles uniform $\text{Ba}_{0.2}\text{Sr}_{0.2}\text{La}_{0.6}\text{MnO}_3$ is as shown in Figure 4a with average size 60 to 120 nm. According to Figure 4b, MWCNT/NPs composite by 10% wt MWCNTs indicated that high percentage of functionalized MWCNTs is covered by magnetic and hexagonal nanoparticles. The thickness of synthesized MWCNT/NPs is 100 nm. The NPs were grown on MWCNT as well on average that shows 400% growth compared to pure MWCNT which 80 nm is related to nanoparticles. Figure 4c shows FESEM of MWCNT/ $\text{Ba}_{0.2}\text{Sr}_{0.2}\text{La}_{0.6}\text{MnO}_3$ /PANI with full coverage of MWCNT/NPs by PANI. The average thickness of nanocomposite is 135 nm which is evidenced by the growth of PANI layer on MWCNT/NPs. The FESEM images showed NPs are formed in appropriate size and shape uniformity and well-formed NPs are well covered nanotube, PANI is well covered with NPs and carbon nanotube.

Magnetic properties

Magnetic property is determined with respect to loops hysteresis of magnetic properties of nanocomposite MWCNT/NPs/PANI of nanocomposite such as saturation magnetization (M_s), coercivity (H_c), and remnant magnetization (M_r) at various stages of the synthesis in the room temperature with an applied field. The M_r , M_s

and H_c amount are summarized in Table 1. Magnetic hysteresis loops of NPs, MWCNT/NPs and MWCNT/NPs/PANI is as shown in Figure 5a and b.

The remain of coercivity, loop hysteresis and paramagnetic properties of MWCNT/ $\text{Ba}_{0.2}\text{Sr}_{0.2}\text{La}_{0.6}\text{MnO}_3$ /PANI are predictable in the applied magnetic field. PANI as a conductive polymer can reduce magnetic properties of NPs. This material is slightly attracted by magnetic field and do not retain their magnetic state after discontinuation of field, because in this case, random thermal motion causes the random orientation of the spins. Features paramagnetic are due to the number of unpaired electron and new arrangement of the electron paths which arise due to the external magnetic field. Paramagnetic is a form of magnetic materials that some substances are absorbed by the applied external field.

Microwave absorption

The maximum reflection loss (RL), absorption frequency, maximum absorption% and bandwidth at different thickness of paraffin composite (80%wt) are summarized in Table 2. As shown in Table 2, with increase in the thickness of the samples, the absorption percentage and RL increases. On the other hand, we expected the presence of NPs with magnetic properties and MWCNT and PANI due to their electrical properties to increase

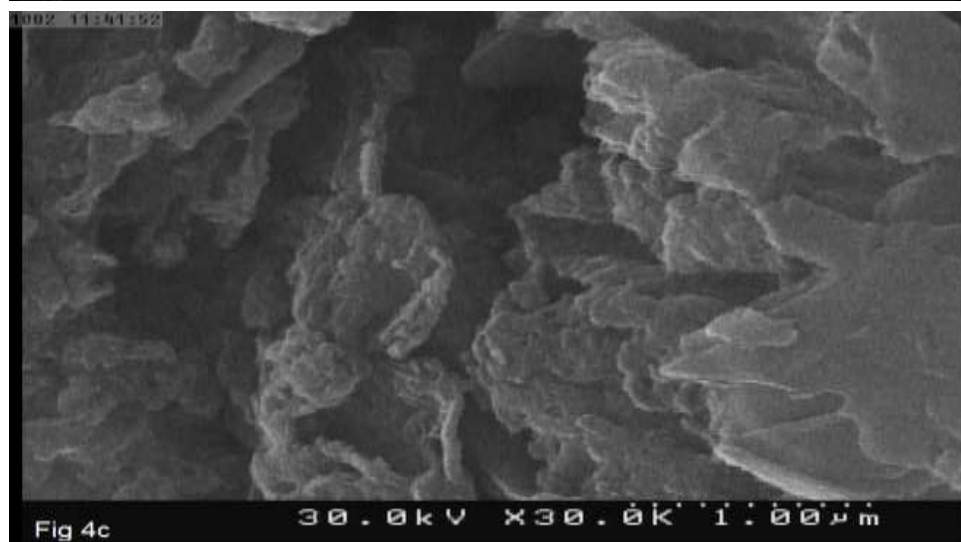
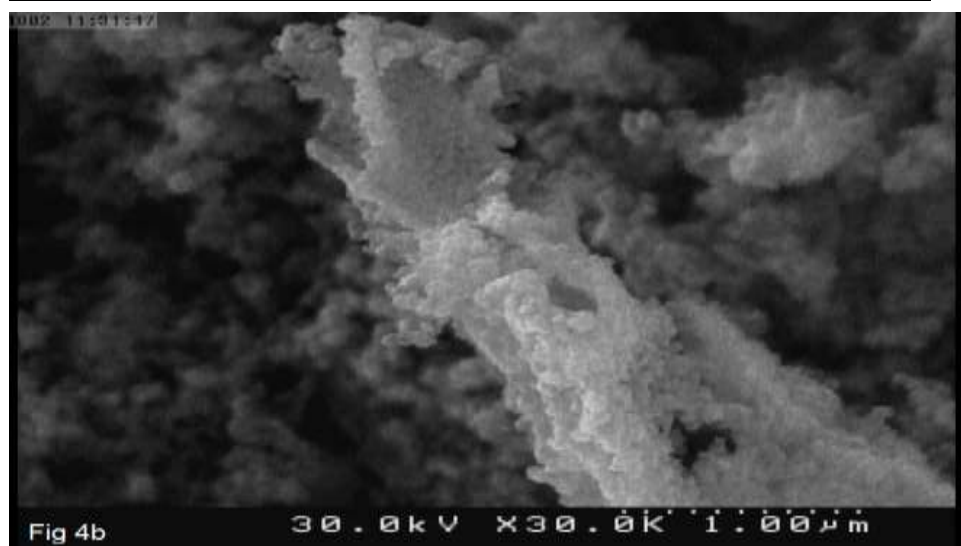
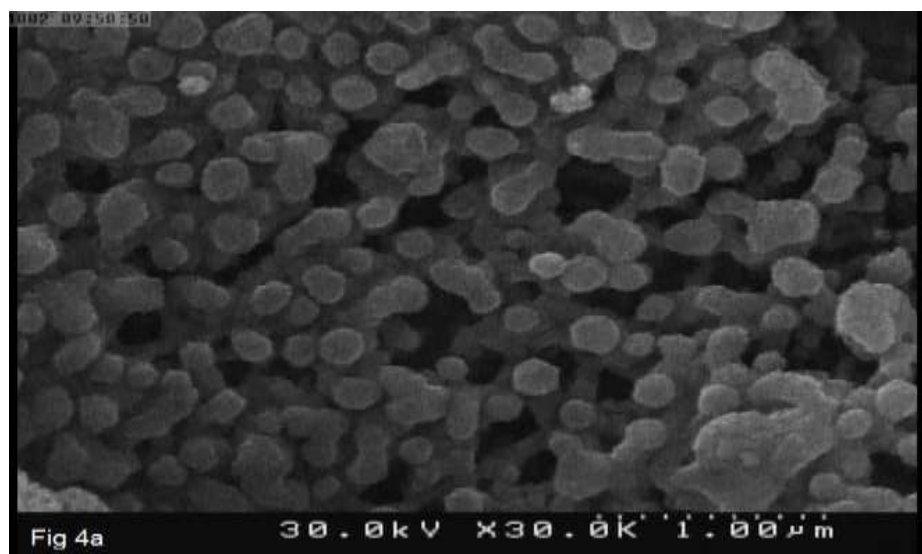


Figure 4. FE-SEM images of (a) $\text{Ba}_{0.2}\text{Sr}_{0.2}\text{La}_{0.6}\text{MnO}_3$ NPs, (b) MWCNT/NPs and (c) MWCNT/NPs/PANI nanocomposites.

Table 1. Magnetic parameters.

Sample	M_s (emu/g)	M_r (emu/g)	H_c (Oe)
$Ba_{0.2}Sr_{0.2}La_{0.6}MnO_3$	10.01	0.36	6.07
MWCNT/ $Ba_{0.2}Sr_{0.2}La_{0.6}MnO_3$	12.06	0.07	2.07
MWCNT/ $Ba_{0.2}Sr_{0.2}La_{0.6}MnO_3$ /PANI	0.01	0.00	177.97

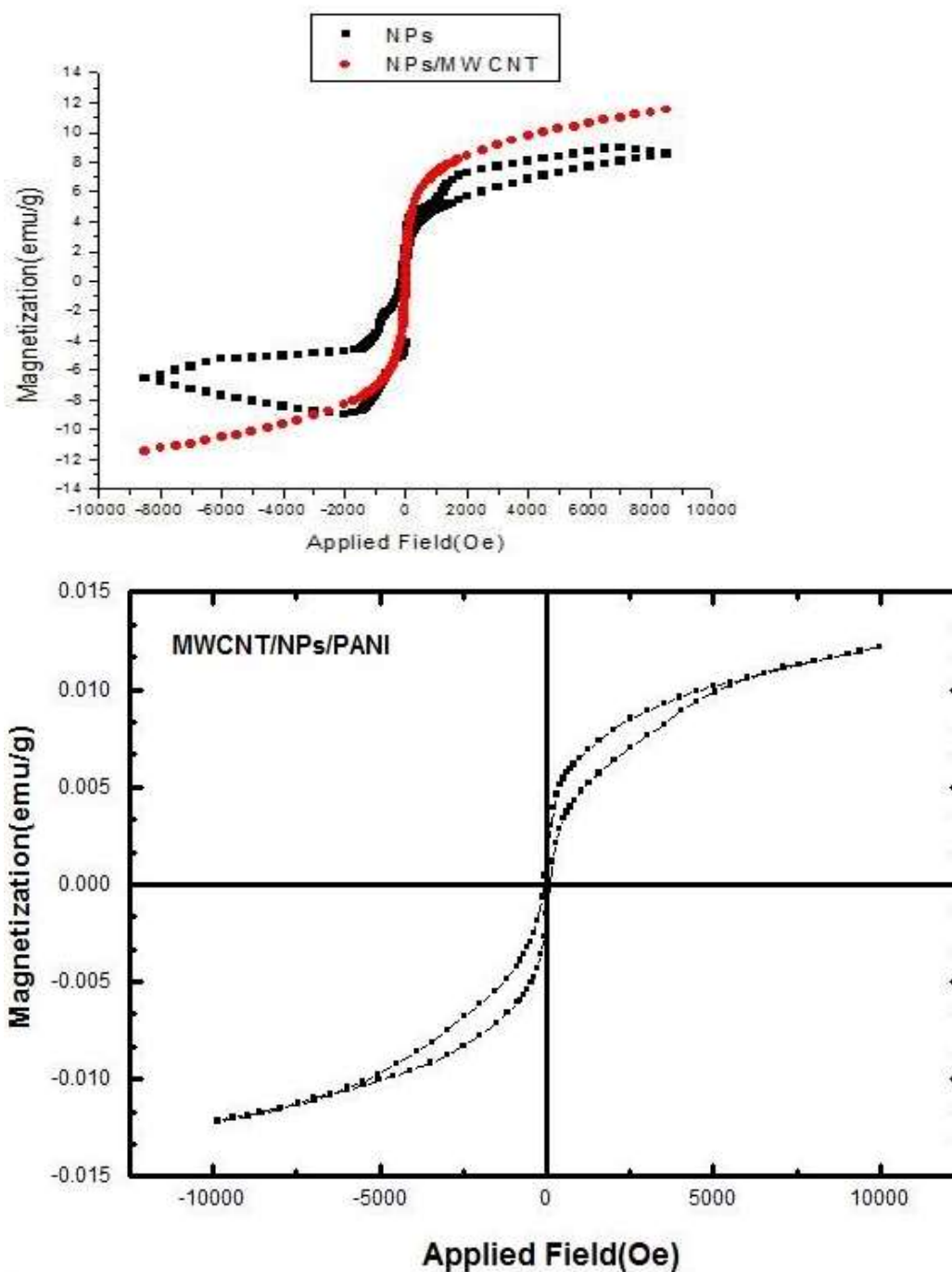
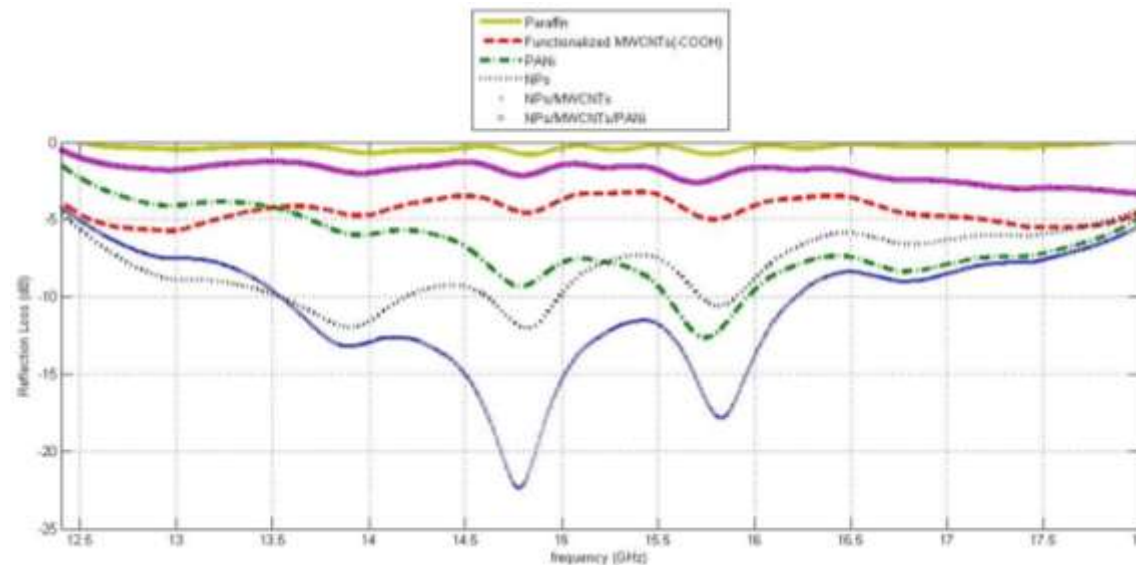


Figure 5. Magnetic hysteresis loops of (a) pure $Ba_{0.2}Sr_{0.2}La_{0.6}MnO_3$ (NPs), $Ba_{0.2}Sr_{0.2}La_{0.6}MnO_3$ /MWCNT and (b) $Ba_{0.2}Sr_{0.2}La_{0.6}MnO_3$ /MWCNT/PANI nano composites.

Table 2. The maximum reflection loss, absorption frequency and bandwidth of the samples at different thickness.

Variable	NPs	NPs	NPs	NPs/MWCNT	NPs/MWCNT	NPs/MWCNT	NPs/MWCNT/PANI
	4.0 mm	5.4 mm	6.5 mm	4.7 mm	5.8 mm	6.5 mm	6.5 mm
Maximum reflection loss (dB)	3.41	11.79	12.04	12.51	22.49	22.36	3.31
Maximum absorption frequency (GHz)	15.59	17.92	14.82	18.00	16.74	14.78	18
Maximum absorption = $1-10^{(-RL/10)}$, %	54.40	93.38	93.75	94.39	99.44	99.42	53.33
Absorption bandwidth (GHz) >5 dB	-	2.69	5.43	2.18	4.12	5.50	-
Absorption bandwidth (GHz) >10 dB	-	0.87	1.22	0.34	2.60	2.67	-
Absorption bandwidth (GHz) >15 dB	-	-	-	-	1.45	0.78	-

**Figure 6.** Reflection loss versus frequency of paraffin, functionalized MWCNTs (-COOH), PANI, $Ba_{0.2}Sr_{0.2}La_{0.6}MnO_3$ /MWCNT/PANI nanocomposite and $Ba_{0.2}Sr_{0.2}La_{0.6}MnO_3$ nanoparticles and $Ba_{0.2}Sr_{0.2}La_{0.6}MnO_3$ /MWCNT nanocomposite with different thickness.

absorption. But with the increase of PANI to composite, contrary to expectations, we see a decrease in the amount of adsorption. This may

be due to the full doping capacity or low molecular weight of the polymer.

Figure 6 shows the microwave absorption

performance of pure paraffin, pure PANI, functionalized MWCNTs (-COOH), NPs, MWCNTs/NPs and MWCNTs/NPs/PANI nanocomposite

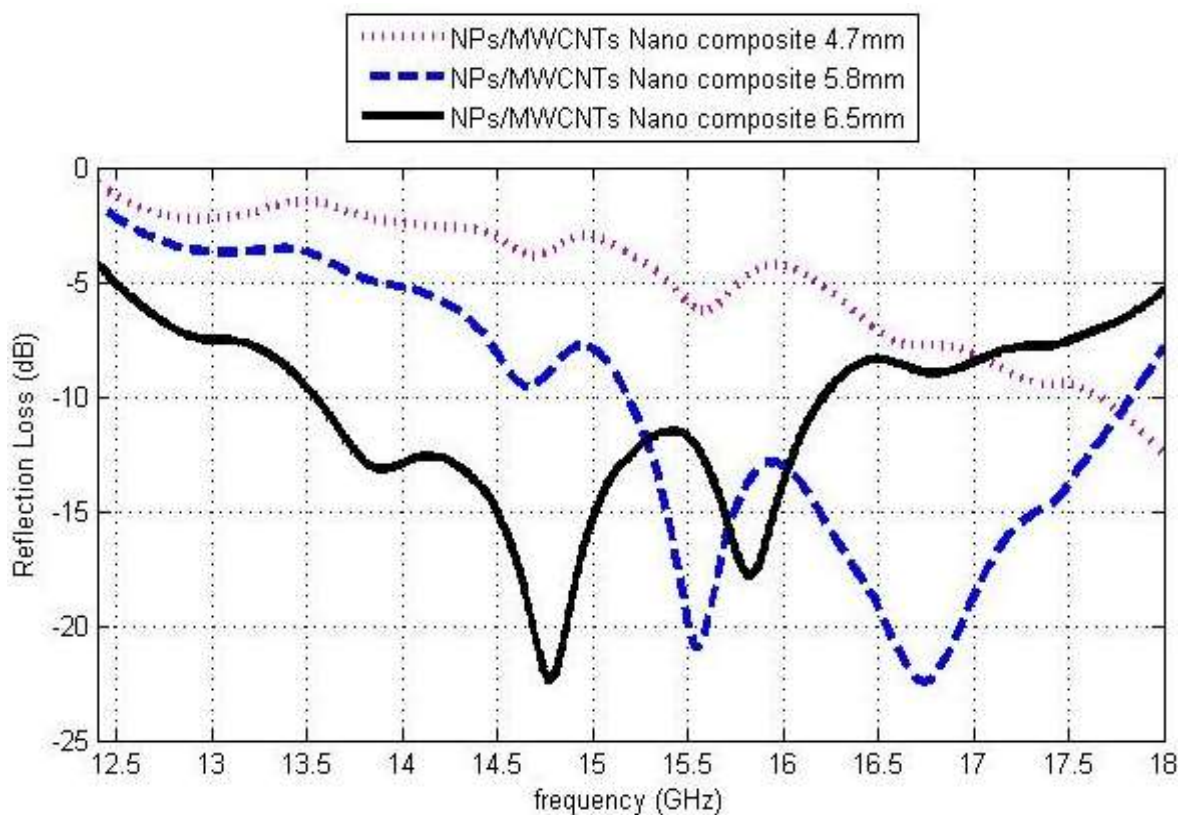


Figure 7. Reflection loss versus frequency of $\text{Ba}_{0.2}\text{Sr}_{0.2}\text{La}_{0.6}\text{MnO}_3$ with different thickness.

in 6.5 mm thickness. PANI as conductive polymer and functional MWCNTs (-COOH) showed electromagnetic behavior expected in microwave absorption with its electrical properties. The maximum reflection loss of the $\text{Ba}_{0.2}\text{Sr}_{0.2}\text{La}_{0.6}\text{MnO}_3$ NPs was about -12.04 dB at 14.82 GHz with a bandwidth of 1.22 GHz ($\text{RL} < -10$ dB). The maximum reflection loss of the MWCNT/ $\text{Ba}_{0.2}\text{Sr}_{0.2}\text{La}_{0.6}\text{MnO}_3$ was about -22.36 dB at 14.78 GHz with a bandwidth of 2.67 GHz ($\text{RL} < -10$ dB). Functionalized MWCNTs (-COOH) (10%Wt) with a hollow structure as a disperser agent increase the quality of the synthesized nanoparticles on one hand and increase the electrical properties of composites in the presence of MWCNTs.

On the other hand, improves the absorption of the microwave. However, in the presence of 80% wt PANI composite NPs/MWCNTs in frequency 12-18 GHz (Ku band) increases the electrical properties of the composite which has not effect on microwave absorption. The reason can be shifted to higher frequencies as the maximum absorption of microwave. The curves reflection loss of $\text{Ba}_{0.2}\text{Sr}_{0.2}\text{La}_{0.6}\text{MnO}_3$ and MWCNT/ $\text{Ba}_{0.2}\text{Sr}_{0.2}\text{La}_{0.6}\text{MnO}_3$ are as shown in Figures 7 and 8, with different thickness, respectively. Increasing thickness of

samples, maximum absorption will be increased. By reducing the thickness of the absorbent, maximum absorption (RL) shifted towards higher frequencies.

Conclusion

The electromagnetic waves absorption study showed that nanocomposites have attracted at different stages and different synthesis methods in appropriate range and carbon nanotube reinforced magnetic waves. According to the results, we can conclude that functional MWCNTs were coated with NPs by sol-gel method. MWCNTs with increase in di-electric properties of nanoparticles along magnetic properties increased maximum absorption of microwave and absorption bandwidth. The MWCNTs/NPs increased maximum absorption of microwave and bandwidth. Since the magnetic nanoparticles have low environmental sustainability, is not able to use the microwave absorbing materials alone. We need to have a polymeric substrate. PANI is one of the best candidates because of conductivity which have the ability to absorb wave due to the high stability in terms of doping and non-doping, high resistance to heat and ease of reform. PANI

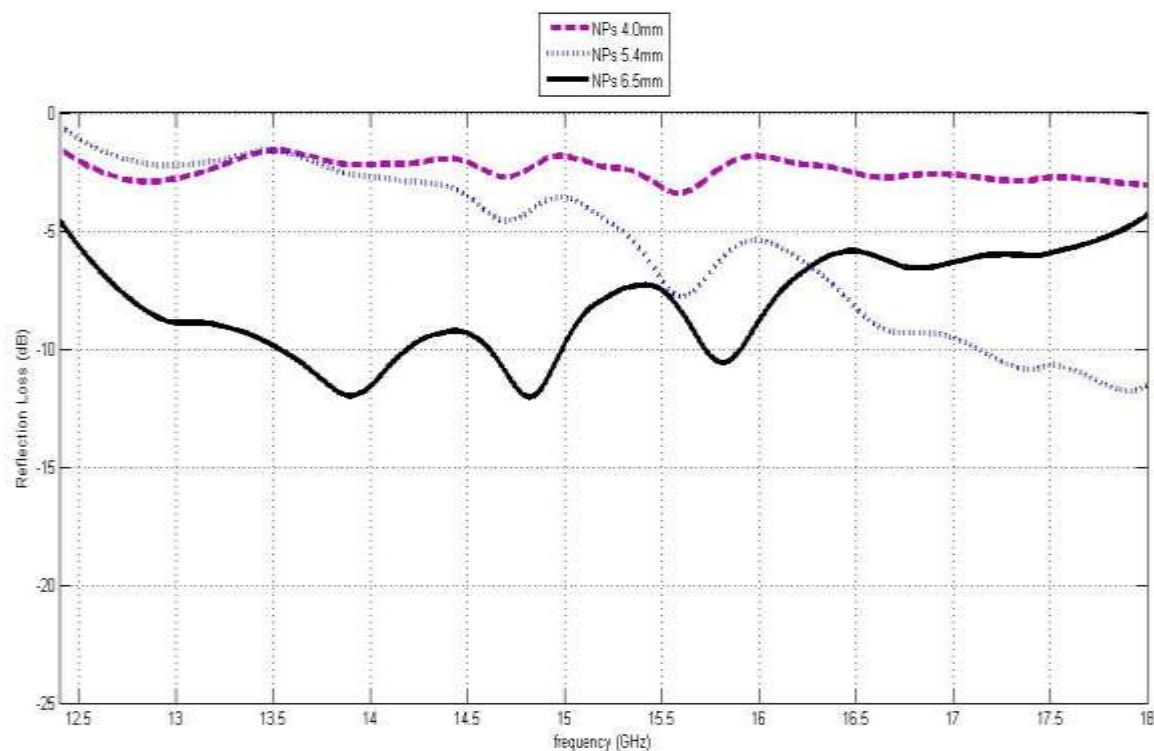


Figure 8. Reflection loss versus frequency of MWCNT/Ba_{0.2}Sr_{0.2}La_{0.6}MnO₃ with different thickness.

as conductive polymer with di-electric properties is a good absorbent for microwaves alone. Results indicated that MWCNT and conducting polymers with magnetic nanoparticles enhance microwave absorption peak width in 12 to 18 GHz.

CONFLICT OF INTERESTS

The authors have not declared any conflict of interests.

REFERENCES

- Acharya S, Datar S (2020). Wideband (8–18 GHz) microwave absorption dominated electromagnetic interference (EMI) shielding composite using copper aluminum ferrite and reduced graphene oxide in polymer matrix. *Journal of Applied Physics* 128:104902, 1-11.
- Amiri G (2019). Structural, Magnetic and Microwave Absorption Properties of Ba_{0.5}Sr_{0.5}Ni_{2-x}(MgZn)_{x/2}Fe₁₆O₂₇ Hexaferrite Nanoparticles Prepared by the Sol-Gel Combustion Method. *Journal of Superconductivity and Novel Magnetism*, 32:957-961.
- Ban I, Stergar J, Maver U (2018). NiCu magnetic nanoparticles: review of synthesis methods, surface functionalization approaches, and biomedical applications. *Nanotechnology Reviews* 7(2):187-207.
- Banerjee J, Dutta K (2019). Melt-mixed carbon nanotubes/polymer nanocomposites. *Polymer Composites* 40(12):4473-4488.
- Bezzon VDN, Montanheiro TLA, De Menezes BRC, Ribas RG, Righetti VAN, Rodrigues KF, Thim GP (2019). Carbon Nanostructure-based Sensors: A Brief Review on Recent Advances, *Advances in Materials Science and Engineering* 2019:1-21.
- Biswas S, Muzata TS, Krause B, Rzeczkowski P, Pötschke P, Bose S (2020). Does the Type of Polymer and Carbon Nanotube Structure Control the Electromagnetic Shielding in Melt-Mixed Polymer Nanocomposites. *Journal of Composites Science* 4(1):9.
- Dolabi MB, Azimi A, Hosseini SH (2020). Preparation of thermal infrared and microwave absorber using WO₃/MnFe₃O₄/polyaniline nanocomposites, *Materials Research Innovations* 24:326-334.
- Donescu D, Corobea MC, Spataru CI, Ghiurea M (2017). Polymer-carbon nanotubes composites obtained via radical polymerization in water-dispersed media. *Hybrid Polymer Composite Materials* pp. 281-305.
- Green M, Xiaobo C (2019). Recent progress of nanomaterials for microwave absorption. *Journal of Materiomics* 5(4):503-541.
- Gómez NT, Nava O, Figueroa LA, Contreras RG, Barrera AB, Vilchis-Nestor AR (2019). Shape Tuning of Magnetite Nanoparticles Obtained by Hydrothermal Synthesis: Effect of Temperature. *Journal of Nanomaterials* 2019:1-15.
- Ibanez JG, Rincon AE, Granados SG, Chahma M, Quintero OAG, Uribe BAF (2018). Conducting Polymers in the Fields of Energy, Environmental Remediation, and Chemical-Chiral Sensors. *Chem Rev* 118(9):4731-4816.
- Hosseini SH, Zamani P (2016a). Preration of thermal infrared and microwave absorber using SrTiO₃/BaFe₁₂O₁₉/Polyaniline nanocomposites. *Journal of Magnetism and Magnetic Materials* 397:205-212.
- Hosseini SH, Alamian A, Mousavi SM (2016b). Preparation of magnetic and conductive graphite nanoflakes/SrFe₁₂O₁₉/polythiophene. *Fibers and Polymers* 17:593-599.
- Hosseini SH, Tarakameh M, Hosseini SS (2020a). Preparation of thermal neutron absorber based B₄C/TiO₂/polyaniline nanocomposite. *International Journal of Physical Sciences* 15(2):49-59.

- Hosseini SH, Azimi A, Dolabi MB (2020b). Study of UV-Visible and near infrared absorption CsXWO₃/polypyrrole nanocomposite. *Materials Research Innovations*, 24:335-340.
- Mei W, Xiaosi Q, Ren X, Zhongchen B, Shuijie Q, Wei Z, Chaoyong D (2020). Graphene oxide/carbon nanotubes/Co_xFe_{3-x}O₄ ternary nanocomposites: Controllable synthesis and their excellent microwave absorption capabilities. *Journal of Alloys and Compounds* 813:151996.
- Minin RV, Itin VI, Zhuravlev VA, Svetlichnyi VA (2018). Synthesis of cubic ferrite CoFe₂O₄ by spray pyrolysis. *Journal of Physics: Conf Series* 1115:042011-5.
- Mishra AK (2018). Conducting Polymers: Concepts and Applications. *Journal of Atomic, Molecular, Condensate & Nano Physics* 5(2):159-193.
- Rao R, Pint CL, Islam AE, Hofmann S, Meshot ER (2018). Carbon Nanotubes and Related Nanomaterials: Critical Advances and Challenges for Synthesis toward Mainstream Commercial Applications. *ACS Nano* 12:11756-11784.
- Sen G, Islam SN, Banerjee A, Das S (2017). Broadband perfect metamaterial absorber on thin substrate for X-band and Ku-band applications. *Progress in Electromagnetics Research C* 73:9-16.